Stem Cell Research 48 (2020) 101962

Contents lists available at ScienceDirect

Stem Cell Research

journal homepage: www.elsevier.com/locate/scr

CRISPR/Cas9 editing to generate a heterozygous *COL2A1* p.G1170S human chondrodysplasia iPSC line, MCRIi019-A-2, in a control iPSC line, MCRIi019-A

Louise H.W. Kung[a], Lisa Sampurno[a], Kathryn M. Yammine[c], Alison Graham[a], Penny McDonald[a], John F. Bateman[a,b,*], Matthew D. Shoulders[c,*], Shireen R. Lamandé[a,b]

[a] *Murdoch Children's Research Institute, Australia*
[b] *Department of Paediatrics, University of Melbourne, Australia*
[c] *Department of Chemistry, Massachusetts Institute of Technology, USA*

A B S T R A C T

To develop an *in vitro* disease model of a human chondrodysplasia, we used CRISPR/Cas9 gene editing to generate a heterozygous *COL2A1* exon 50 c.3508 GGT > TCA (p.G1170S) mutation in a control human iPSC line. Both the control and *COL2A1* mutant lines displayed typical iPSC characteristics, including normal cell morphology, expression of pluripotency markers, the ability to differentiate into endoderm, ectoderm and mesoderm lineages and normal karyotype. These chondrodysplasia mutant and isogenic control cell lines can be used to explore disease mechanisms underlying type II collagenopathies and aid in the discovery of new therapeutic strategies.

1. Resource Table

Unique stem cell line identifiers	MCRIi019-A MCRIi019-A-2
Alternative names of stem cell lines	1502.3 (MCRIi019-A) 1502.3 *COL2A1* p.G1170S (MCRIi019-A-2)
Institution	Murdoch Children's Research Institute, Melbourne, Australia and Massachusetts Institute of Technology, USA
Contact information of distributor	Associate Professor Shireen Lamandé shireen.lamande@mcri.edu.au; Associate Professor Matthew Shoulders mshoulde@mit.edu
Type of cell lines	iPSC
Origin	Human
Cell Source	Dermal fibroblast-derived human induced pluripotent cell line MCRIi019-A (http://hpscreg.eu/cell-line/MCRIi019-A)
Clonality	Clonal
Method of reprogramming	Episomal vectors
Multiline rationale	Isogenic clones
Gene modification	Yes
Type of modification	Induced mutation
Associated disease	Legg-Calve-Perthes Disease OMIM #150600
Gene/locus	*COL2A1* c.3508 GGT > TCA (p.G1170S) Chromosome 12q13.11
Method of modification	CRISPR/Cas9
Name of transgene or resistance	N/A
Inducible/constitutive system	N/A
Date archived/stock date	February 2019
Cell line repository/bank	https://hpscreg.eu/cell-line/MCRIi019-A; https://hpscreg.eu/cell-line/MCRIi019-A-2
Ethical approval	This study was approved through the Human Research Ethics Committee of the Royal Children's Hospital (HREC 33118), Victoria, Australia

* Corresponding authors at: Murdoch Children's Research Institute, Parkville, Victoria 3052, Australia (J.F. Bateman); Department of Chemistry, Massachusetts Institute of Technology, 77 Massachusetts Avenue, 16-573A, Cambridge, MA 02139, USA (M.D. Shoulders).
E-mail addresses: john.bateman@mcri.edu.au (J.F. Bateman), mshoulde@mit.edu (M.D. Shoulders).

https://doi.org/10.1016/j.scr.2020.101962
Received 30 June 2020; Received in revised form 3 August 2020; Accepted 22 August 2020
Available online 06 September 2020

2. Resource utility

This chondrodysplasia iPSC line (*COL2A1* p.G1170S), together with its parental isogenic control line, provide an *in vitro* human disease model to study the pathological mechanisms underlying this type II collagenopathy and explore new therapeutic strategies.

3. Resource details

Collagen type II is the most abundant structural protein of cartilage extracellular matrix. Autosomal-dominant mutations in the gene encoding the α1 chain of procollagen type II (*COL2A1*) result in a clinically wide spectrum of chondrodysplasias, collectively termed type II collagenopathies. These disorders range from mild to severe and perinatal lethal skeletal phenotypes (http://databases.lovd.nl/shared/genes/COL2A1). Although clinically variable, abnormal growth plate morphology and delayed endochondral ossification are commonly reported. The most common *COL2A1* mutations are heterozygous dominant negative missense mutations that disrupt the assembly or structural integrity of the collagen II protein triple helix. To gain insights into the relationship between mutant collagen II and altered cartilage development, we generated a human iPSC line with a heterozygous patient *COL2A1* mutation (*COL2A1* exon 50 c.3508 GGT > TCA; p.G1170S) causing Legg-Calve-Perthes disease (OMIM #150600), a form of Avascular Necrosis of Femoral Head (OMIM #608805) found in growing children. The resulting bone deformity results in precocious osteoarthritis of the hip. A homozygous *Col2a1* p.G1170S mouse model accumulates misfolded procollagen in the endoplasmic reticulum, activating a stress response and apoptosis in the growth plate cartilage, disrupting normal chondrogenesis (Liang et al., 2014). This provides some mechanistic clues, but because the mouse model has a homozygous mutation, it does not faithfully replicate the human disease. Our heterozygous human iPSC mutant line, together with the parental isogenic control line (Table 1), will provide a more accurate *in vitro* human cartilage disease model to help unravel the pathological mechanisms underlying type II collagenopathies and test new therapeutic approaches.

A control human iPSC line, MCRIi019-A, derived from dermal fibroblasts (ATCC cat: CRL-1502; http://hpscreg.eu/cell-line/MCRIi019-A), was co-transfected with Cas9-gem mRNA, a plasmid encoding a *COL2A1*-specific sgRNA, and a 170 bp oligodeoxynucleotide (ODN) repair template comprising ~80 bp homology arms flanking the codon mutation (Fig. 1A) two days post-passaging. Individual iPSC colonies were isolated, expanded and screened by PCR using an allele specific primer that overlaps the 3 bp changes incorporated in the ODN. The heterozygous *COL2A1* c.3508 GGT > TCA mutation in genomic DNA and transcribed mRNA in clone MCRIi019-A-2 was confirmed by Sanger sequencing (Fig. 1B).

Both the control and gene-edited iPSC lines, MCRIi019-A and MCRIi019-A-2 respectively, displayed normal stem cell morphology, characterised by compact colonies with well-defined boundaries and a high nucleus to cytoplasm ratio (Fig. 1C). Immunofluorescent staining confirmed co-expression of the pluripotency markers OCT4 and NANOG in both cell lines (Fig. 1C). Flow cytometry showed that both cell lines strongly express the pluripotency markers OCT3/4, SSEA4 and TRA-1-60 (Fig. 1D). Both iPSC lines could differentiate into the three main germ layers. Directed differentiation to definitive endoderm was confirmed by the expression of endoderm marker SOX17 (Fig. 1E). *SOX9*, *COL2A1*, *MEOX1* and *FOXC2* expression confirmed differentiation into sclerotome, a mesoderm derivative (Fig. 1F). Lastly, neuroectoderm differentiation was demonstrated by co-expression of Nestin and PAX6 (Fig. 1G).

Genome SNP array analysis of both lines confirmed no aneuploidies or large deletions or insertions (Supplementary Fig. 1). It should be noted that the SNP analysis does not preclude the presence of balanced translocations. SNP Duo analysis also confirmed that MCRIi019-A-2 had > 99.9% identity to the parental line MCRIi019-A (Table 2, Supplementary Fig. 1). Both lines were confirmed to be free from mycoplasma contamination (Table 2, Supplementary Fig. 1).

4. Materials and methods

4.1. Cell culture

MCRIi019-A and MCRIi019-A-2 cells were cultured at 37 °C with 5% CO_2 on Matrigel (Corning)-coated plates in Essential 8 (E8) medium (Thermo Fisher Scientific). Media was changed daily and cells were passaged (1:4 – 1:6) every 3–4 days with 0.5 mM EDTA in PBS.

4.2. CRISPR/Cas9-mediated gene editing

The sgRNA to target *COL2A1* was designed using a CRISPR design tool (http://crispr.mit.edu/). The sgRNA oligonucleotides were annealed and ligated into pSMART-sgRNA (Sp) plasmid (Addgene # 80427) then sequenced to confirm that errors had not been introduced. Control MCRIi019-A iPSCs were harvested with TrypLE (Thermo Fisher Scientific) 2 days after passaging and resuspended in Buffer R at a final concentration of 1×10^7 cells/ml. For electroporation with the Neon® Transfection System (Thermo Fisher Scientific, 1100 V, 30 ms, 1 pulse) 100 µl of the cell suspension was added to a tube containing 5 ug of *in vitro* transcribed Cas9gem mRNA, 2 µg pSMART-COL2A1-sgRNA plasmid and 10 µM of the oligodeoxynucleotide (ODN) repair template incorporating the mutation (Integrated DNA Technologies) (Howden et al., 2018). Electroporated cells were plated over 4 wells of a Matrigel-coated 6-well plate in E8 medium with 10 µM ROCK inhibitor, Y-27632 (Tocris). The medium was switched to E8 without Y-27632 the next day and changed every other day. Individual colonies were isolated and expanded in E8 medium.

Table 1
Summary of lines.

iPSC line names	Abbreviation in figures	Gender	Age	Ethnicity	Genotype of locus	Disease
MCRIi019-A		Female	12 weeks gestation	Black	*COL2A1*	Normal
MCRIi019-A-2		Female	12 weeks gestation	Black	*COL2A1* c.3508 GGT > TCA	Type II Collagenopathy; Legg-Calve-Perthes disease (OMIM #150600)

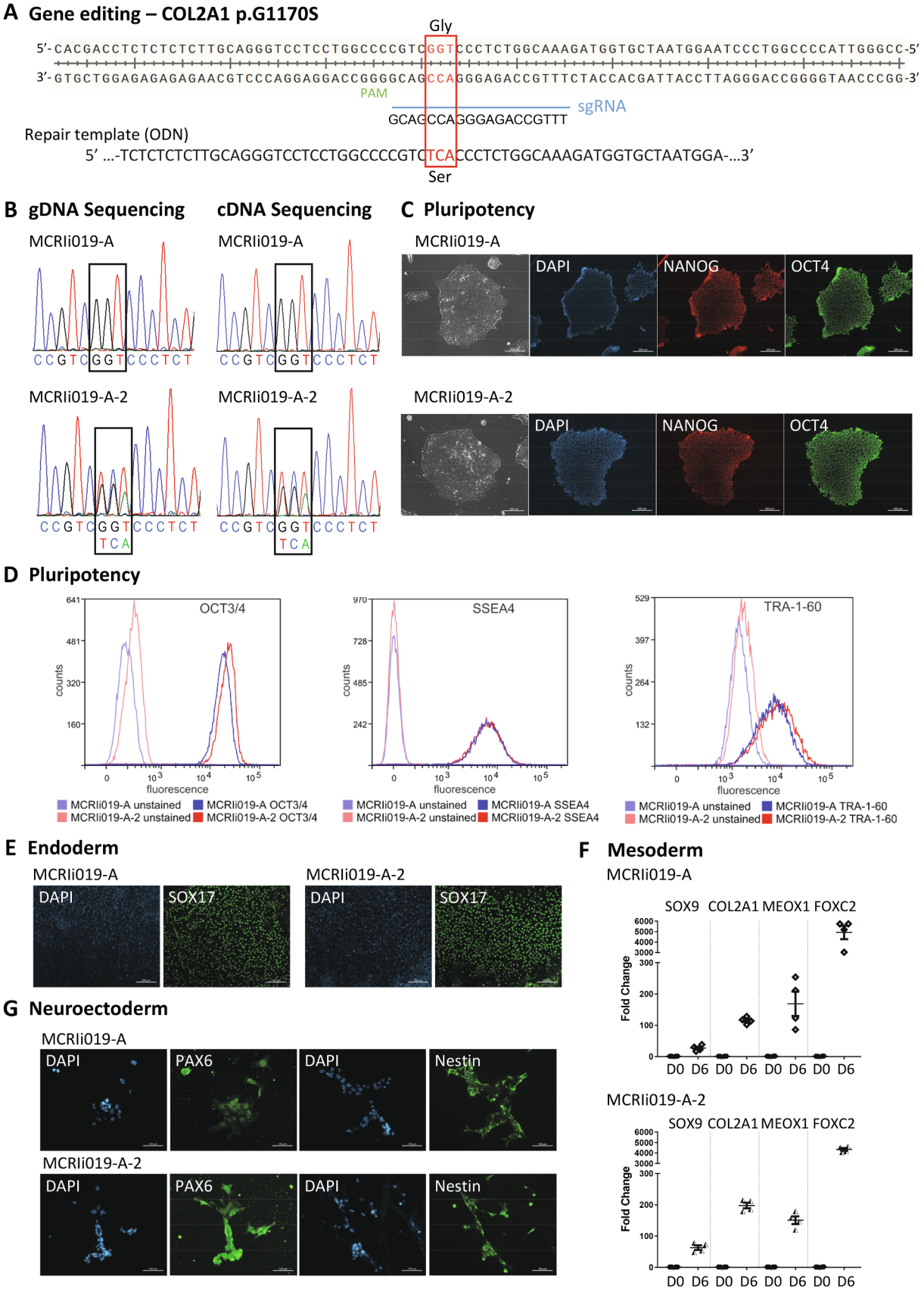

Fig. 1. Molecular and cellular characterization.

Table 2
Characterization and validation.

Classification	Test	Result	Data
Morphology	Photography	Normal	Fig. 1, panel C
Phenotype	Qualitative analysis	OCT4 and NANOG positive staining	Fig. 1, panel C
	Quantitative analysis	MCRIi019-A: TRA-1-60: 73.41% SSEA4: 99.67% OCT3/4: 99.57% MCRIi019-A-2: TRA-1-60: 78.71% SSEA4: 98.85% OCT3/4: 98.93%	Fig. 1, panel D
Genotype	Molecular Karyotype and resolution	arr(1–22,X)x2 Resolution: 0.5 Mb	Supplementary Fig. 1
Identity	SNPDuo analysis of SNParrays	Identical genotypes (> 99.9%) for the entire genome, indicating the lines are from the same individual	Supplementary Fig. 1
Mutation analysis	Sequencing	Heterozygous COL2A1 c.3508 GGT > TCA mutation confirmed in MCRIi019-A-2	Fig. 1, panel B
Microbiology and virology	Mycoplasma	Mycoplasma testing by PCR. Both lines confirmed negative	Supplementary Fig 2
Differentiation potential	Directed differentiation	Endoderm: SOX17 Ectoderm: Nestin and PAX6 Mesoderm: MEOX1, FOXC2, SOX9, COL2A1	Fig. 1, panels E-G
Donor screening	HIV 1 + 2 Hepatitis B, Hepatitis C	N/A	N/A
Genotype additional info	Blood group genotyping	N/A	N/A
	HLA tissue typing	N/A	N/A

4.3. PCR screening and sequencing

Potentially targeted clones were screened using allele-specific PCR primers that could only bind the correctly targeted *COL2A1* G1170S mutation. gDNA was extracted using a DNAeasy Blood and Tissue Kit (Qiagen) according to the manufacturer's instructions. PCR used GoTaq Green Mastermix (Promega) with primer sets specified in Table 3 and an Applied Biosystems (Veriti) 96-well thermocycler. PCR conditions were 95 °C for 3 min, followed by 35 cycles of 95 °C for 18 s, 55 °C for 18 s, 72 °C for 40 s, and then 72 °C for 5 min. PCR products were analysed by agarose gel electrophoresis. PCR products using primers that flank the *COL2A1* G1170S mutation site were generated (Table 3) and the antisense strand was Sanger-sequenced to confirm the mutation, clonality and/or absence of indel mutations. To confirm the mutation at the mRNA level, RNA and cDNA were prepared as described below. The cDNA was PCR amplified and sequenced using the BigDye Terminator v3.1 cycle sequencing kit (Thermo Fisher Scientific).

4.4. Quantitative RT-PCR

RNA was extracted using TRIzol (Invitrogen) and reverse transcribed using the QuantiTect® Reverse Transcription Kit (Qiagen). Brilliant III Ultra-Fast SYBR®Green QPCR Master Mix (Agilent Technologies) and gene-specific primers were used for qPCR (Table 3).

4.5. Immunocytochemistry

Cells were fixed in 4% paraformaldehyde then permeabilized with 0.05% Triton X-100 in PBS for 10 min at 4 °C. Non-specific binding was blocked with 3% bovine serum albumin in 0.1% PBST for 30 min at room temperature. Cells were incubated with primary antibodies at 4 °C overnight, followed by secondary antibodies for 60 min at room temperature (Table 3). Nuclei were stained with DAPI (1 μg/ml) and cells visualised with an Olympus IX70 fluorescent microscope.

4.6. Flow cytometry

Cells were dissociated with TrypLE (Thermo Fisher Scientific) and incubated with conjugated antibodies to cell surface proteins TRA-1-60 and SSEA4 (Table 3) diluted in PBS containing 2% fetal bovine serum (FBS) for 15 min at 4 °C. Cells were washed with 2% FBS in PBS, then fixed and permeabilized using the eBioscience™ Foxp3/Transcription Factor Staining buffer set (Thermo Fischer Scientific), then stained with a conjugated antibody to intracellular OCT3/4 (Table 3). Samples were analysed using a LSR Fortessa X20 (BD Biosciences) and BD FACSDiva and FCS Express software.

4.7. Directed differentiation

iPSCs were differentiated in monolayer culture into definitive endoderm for 5 days (Loh et al., 2014), anterior neuroectoderm for 12 days (Tchieu et al., 2017) and sclerotome for mesodermal potential for 6 days (Loh et al., 2016). Differentiation was assessed by immunocytochemistry and/or qPCR for lineage-specific markers.

4.8. Molecular karyotyping and SNP analysis

Cell pellets (MCRIi019-A passage 10, MCRIi019-A-2 passage 26) were provided to the Victorian Clinical Genetics Service (Murdoch Children's Research Institute, Melbourne, Australia) and genomic DNA was analysed using an Infinium GSA-24 v1.0 SNP array (Illumina).

4.9. Mycoplasma detection

Absence of mycoplasma contamination was confirmed by PCR by the commercial service provider Cerberus Sciences (Adelaide, Australia).

Table 3
Reagent details.

Antibodies used for immunocytochemistry/flow-cytometry			
	Antibody	**Dilution**	**Company Cat # and RRID**
Pluripotency Marker	Oct-4A (C30A3) Rabbit Monoclonal Antibody	1:400	Cell Signaling Technology Cat# 2840S, RRID: AB_2167691
Pluripotency Marker	Purified anti-Nanog Antibody	1:200	BioLegend Cat# 674202, RRID: AB_2564574
Endoderm Marker	Human Sox17 Antibody	1:100	R&D Systems Cat# AF1924, RRID:AB_355060
Neuroectoderm Marker	PAX6 Monoclonal Antibody (13B10-1A10)	1:200	Thermo Fisher Scientific Cat#MA1-109; RRID: AB_2536820
Neuroectoderm Marker	Anti-Nestin Antibody, clone 10C2	1:200	Merck Cat# MAB5326, RRID: AB_2251134
Secondary Antibody	Donkey anti-Mouse IgG (H + L) Highly Cross-Adsorbed Secondary Antibody, Alexa Fluor 594	1:1000	Thermo Fisher Scientific Cat# A21203, RRID: AB_2535789
Secondary Antibody	Goat anti-Rabbit IgG (H + L) Cross-Adsorbed Secondary Antibody, Alexa Fluor 488	1:1000	Thermo Fisher Scientific Cat# A11008, RRID: AB_143,165
Secondary Antibody	Donkey Anti-Goat IgG H&L (Alexa Fluor® 594)	1:1000	Abcam Cat# ab150132, RRID:AB_2810222
Secondary Antibody	Goat anti-Mouse IgG (H + L) Highly Cross-Adsorbed Secondary Antibody, Alexa Fluor 488	1:1000	Thermo Fisher Scientific Cat# A11029; RRID: AB_2534088
FACS antibody	BV421 Mouse Anti-Human TRA-1–60 Antigen	1:20	Becton Dickinson Cat# 562711, RRID: AB_2737738
FACS antibody	Alexa Fluor 647 anti-human SSEA-4 antibody	1:100	BioLegend Cat# 330408, RRID: AB_1089200
FACS antibody	PE Mouse anti-Oct3/4	1:5	BD Biosciences Cat# 560186, RRID: AB_1645331

Primers		
	Target	**Forward/Reverse primer (5′-3′)**
sgRNA	*COL2A1* exon 50	TTTGCCAGAGGGACCGACG/ CGTCGGTCCCTCTGGCAAA
Repair Template (ODN) Sequence (Mutation bolded)	*COL2A1* intron 49-intron 50	CCAGCGACTCCCCAGCCTTCCCTGTGGTGACCACTC TTTCCTCACGACCTCTCTCTCTTGCAGGGTCCTCCTG GCCCCGTC**TCA**CCCTCTGGCAAAGATGGTGCTAATG GAATCCCTGGCCCCATTGGGCCTCCTGGTCCCCGTG GACGATCAGGCGAAACCGGCCCTGC
COL2A1-1170mut – mutation screening PCR	*COL2A1* intron 49-exon 50	ACAAACATGAATCAGCCTCTCG/ CATCTTTGCCAGAGGGTGAG
COL2A1-1170scr – PCR for gDNA sequencing	*COL2A1* intron 49- intron 50	ACAAACATGAATCAGCCTCTCG/ CAGCAGGAAACAGAGAGATCAGC
COL2A1-1170 gDNA seqR – gDNA sequencing	*COL2A1* intron 50	AGCCAGGATTGTGTGAAAGTGC
COL2A1 cDNA Seq – RT-PCR and sequencing	*COL2A1* exon 48–51	CCCAGAGGTGACAAAGGAGA/ AGGGACTTGAGTGTGGCATC
Cartilage marker – quantitative RT-PCR	SOX9	AAGTCGGTGAAGAACGGGC/ TCTCGCTTCAGGTCAGCCTT
Cartilage marker - quantitative RT-PCR	COL2A1	TCACGTACACTGCCCTGAAG/ GCCCTATGTCCACACCGAAT
Sclerotome marker - quantitative RT-PCR	MEOX1	ACTCGGCTCCGCAGATATGA/ GAACTTGGAGAGGCTGTGGA
Sclerotome marker - quantitative RT-PCR	FOXC2	TGGTATCTCAACCACAGCGG/ CCCGGGACACGTCAGTATTT
Housekeeping gene - quantitative RT-PCR	ACTB	AAGTCCCTTGCCATCCTAAAA/ ATGCTATCACCTCCCCTGTG

Declaration of Competing Interest

The authors declare that they have no known competing financial interests or personal relationships that could have appeared to influence the work reported in this paper.

Acknowledgements

This study was funded by a research grant from The G. Harold and Leila Y. Mathers Foundation, National Health & Medical Research Council, Australia (GNT1146952, GNT1146902), and the Victorian Government's Operational Infrastructure Support Program. The hiPSC line was generated from ATCC®CRL-1502™ fibroblasts by the MCRI Gene Editing Core Facility, which is supported by the Stafford Fox Medical Research Foundation

Appendix A. Supplementary data

Supplementary data to this article can be found online at https://doi.org/10.1016/j.scr.2020.101962.

References

Liang, G., Lian, C., Huang, D., Gao, W., Liang, A., et al., 2014. Endoplasmic reticulum stress-unfolding protein response-apoptosis cascade causes chondrodysplasia in a *col2a1* p.Gly1170Ser mutated mouse model. PLoS ONE 9 (1), e86894.
Howden, S.E., Thomson, J.A., Little, M.H., 2018. Simultaneous reprogramming and gene editing of human fibroblasts. Nat. Protoc. 13, 875–898.
Tchieu, J., Zimmer, B., Fattahi, F., Amin, S., Zeltner, N., Chen, S., Studer, L., 2017. A modular platform for differentiation of human PSCs into all major ectodermal lineages. Cell Stem Cell 21 (399–410), e397.
Loh, K.M., Ang, L.T., Zhang, J., Kumar, V., Ang, J., Auyeong, J.Q., Lee, K.L., Choo, S.H., Lim, C.Y., Nichane, M., Tan, J., Noghabi, M.S., Azzola, L., Ng, E.S., Durruthy-Durruthy, J., Sebastiano, V., Poellinger, L., Elefanty, A.G., Stanley, E.G., Chen, Q.,

Prabhakar, S., Weissman, I.L., Lim, B., 2014. Efficient endoderm induction from human pluripotent stem cells by logically directing signals controlling lineage bifurcations. Cell Stem Cell 14, 237–252.
Loh, K.M., Chen, A., Koh, P.W., Deng, T.Z., Sinha, R., Tsai, J.M., Barkal, A.A., Shen, K.Y., Jain, R., Morganti, R.M., Shyh-Chang, N., Fernhoff, N.B., George, B.M., Wernig, G., Salomon, R.E.A., Chen, Z., Vogel, H., Epstein, J.A., Kundaje, A., Talbot, W.S., Beachy, P.A., Ang, L.T., Weissman, I.L., 2016. Mapping the pairwise choices leading from pluripotency to human bone, heart, and other mesoderm cell types. Cell 166, 451–467.